

## Formation of Zein Microphases in Ethanol–Water

Yi Wang and Graciela W. Padua\*

Department of Food Science and Human Nutrition, University of Illinois at Urbana–Champaign,  
1304 West Pennsylvania Avenue, Urbana, Illinois 61801

Received April 27, 2010. Revised Manuscript Received June 16, 2010

Zein, a major protein of corn, is soluble in binary mixtures of ethanol and water. It has an amphiphilic character and is capable of self-assembly into nano- and microsized rods, spheres, and films upon solvent evaporation. The formation of microspheres is of particular interest for the development of delivery systems. Control over structure formation requires a better understanding of zein behavior in solution. The objective of this work was to investigate the effect of zein concentration and the effect of ethanol–water ratio on the microphase behavior of zein solutions, believed to govern the morphology of microstructures after solvent evaporation. The Flory–Huggins solution theory was applied to model boundary lines between microphases in solution. The study generated information on the zein concentration–ethanol/water ratio conditions where microspheres are formed and provided insight into the microphase behavior of zein ethanolic solutions.

## 1. Introduction

Zein, a major protein of corn, is recognized for its film-forming properties and is under investigation for its potential in the construction of delivery systems for therapeutic and nutritional components. Zein is insoluble in water but readily dispersed in binary mixtures of alcohols and water. It has an amphiphilic character due to its unusual amino acid sequence, which contains over 50% hydrophobic residues.<sup>1</sup> Early studies<sup>2–5</sup> of zein molecular structure estimated that the  $\alpha$ -helix content of zein was between 50 and 60%. Argos and coworkers<sup>6</sup> proposed that zein contains 9–10 identical  $\alpha$ -helix segments. Matsushima and coworkers<sup>7</sup> proposed a structural model where the  $\alpha$ -helical segments were aligned in an antiparallel fashion forming a prism of  $13 \times 1.2 \times 3$  nm in dimension.  $\alpha$ -Helices were connected at each end by glutamine-rich bridges. Accordingly, the prism sides, formed by the outer surface of the helices, were hydrophobic, whereas the top and bottom surfaces of the prism, containing the glutamine-rich bridges, were hydrophilic.<sup>8</sup> Wang and coworkers<sup>9</sup> employed surface plasmon resonance (SPR) to study the hydrophobic/hydrophilic character of zein surfaces. They concluded that the zein molecule contains sharply defined hydrophobic and hydrophilic domains at its surface.

Amphiphilicity is a main driving force for self-assembly.<sup>10</sup> Self-assembly is the spontaneous formation of organized phases from disordered ones. It is mediated by weak interactions, for example,

van der Waals, hydrophobic associations, and hydrogen bonds. Self-assembly gives rise to lyotropic ordered microphases, cubic, hexagonal, gyroid, and lamellar.<sup>11</sup> Zein was observed to form spheres and bicontinuous and lamellar structures upon evaporation of its solvent, aqueous ethanol mixtures, with or without added surfactants.<sup>12</sup> Govor and coworkers<sup>13</sup> suggested that the microstructure of polymer aggregates formed during evaporation of binary solutions can be controlled by varying the concentration of solutes, the type of solvents, and the volume ratio of solvents.

The objective of this work was to investigate the effect of zein concentration and the effect of ethanol–water ratio on the microphase behavior of zein solutions, believed to govern the morphology of evaporation-induced self-assembled structures. The Flory–Huggins solution theory was applied to model boundary lines between microphases. New understanding of zein microphase behavior is expected to guide the development of zein applications, including the formation of microsize spheres for delivery systems.

**1.1. Microphase Behavior.** The mesophase behavior of amphiphilic diblock copolymers has been studied in terms of Flory–Huggins solution theory. Leibler<sup>14</sup> developed a statistical theory of phase equilibria for diblock copolymers with  $\chi N$ , where  $\chi$  is the Flory–Huggins parameter and  $N$  is the polymerization number, and  $f$ , the volume fraction of one of the two monomers, as the only relevant parameters. A phase diagram was constructed where disordered, body-centered-cubic, hexagonal, and lamellar phases were present. An AB diblock copolymer in a mixture of A and B homopolymers acts similarly to an amphiphile in a mixture of oil and water.<sup>15,16</sup> AB diblock copolymers decrease the surface tension between A-rich and B-rich phases.<sup>17,18</sup> Block polymers tend to self-assemble into soft molecular assemblies: spherical or

\*To whom correspondence should be addressed. Tel: 217-333-9336. Fax: 217-333-9329. E-mail: gwpadua@illinois.edu.

(1) Pomes, A. F. *Encyclopedia of Polymer Science and Technology*; Wiley: New York, 1971.

(2) Elliott, M. A.; Williams, J. W. *J. Am. Chem. Soc.* **1939**, *61*, 718–725.

(3) Foster, J. F.; Edsall, J. T. *J. Am. Chem. Soc.* **1945**, *67*, 617–625.

(4) Tatham, A. S.; Field, J. M.; Morris, V. J.; Ianson, K. J.; Cardle, L.; Dufton, M. J.; Shewry, P. R. *J. Biol. Chem.* **1993**, *268*, 26253–26259.

(5) Watson, C. C.; Arrhenius, S.; Williams, J. W. *Nature* **1936**, *137*, 322–323.

(6) Argos, P.; Pedersen, K.; Marks, M. D.; Larkins, B. A. *J. Biol. Chem.* **1982**, *257*, 9984–9990.

(7) Matsushima, N.; Danno, G.; Takezawa, H.; Izumi, Y. *Biochim. Biophys. Acta* **1997**, *1339*, 14–22.

(8) Lai, H. M.; Geil, P. H.; Padua, G. W. *J. Appl. Polym. Sci.* **1999**, *71*, 1267–1281.

(9) Wang, Q.; Wang, J. F.; Geil, P. H.; Padua, G. W. *Biomacromolecules* **2004**, *5*, 1356–1361.

(10) Lowik, D.; van Hest, J. C. M. *Chem. Soc. Rev.* **2004**, *33*, 234–245.

(11) Grason, G. M. *Phys. Rep.* **2006**, *433*, 1–64.

(12) Wang, Q.; Yin, L. L.; Padua, G. W. *Food Biophys.* **2008**, *3*, 174–181.

(13) Govor, L. V.; Parisi, J.; Bauer, G. H.; Reiter, G. *J. Phys.: Condens. Matter* **2009**, *21*, 264015.

(14) Leibler, L. *Macromolecules* **1980**, *13*, 1602–1617.

(15) Holyst, R.; Schick, M. *J. Chem. Phys.* **1992**, *96*, 7728–7737.

(16) Meunier, J.; Langevin, D.; Boccardo, N. *Physics of Amphiphilic Layers*; Springer: Berlin, 1987.

(17) Leibler, L. *Macromolecules* **1982**, *15*, 1283–1290.

(18) Kahlweit, M.; Strey, R.; Firman, P. *J. Phys. Chem.* **1986**, *90*, 671–677.

cylindrical micelles and lamellae.<sup>11</sup> Pryamitsyn and coworkers<sup>19</sup> computed a 2D phase diagram in the  $\chi N$ - $f$  plane for the self-assembly behavior of rod-coil block copolymers. They presented a self-consistent field model where the orientational interactions between the rods were modeled through a Maier-Saupe interaction, whereas the enthalpic interaction between rods and coils was modeled through a standard Flory-Huggins approach. Zein, also an amphiphile, is believed to have a similar phase behavior to diblock copolymers when in aqueous ethanol mixtures. In this work, Flory-Huggins solution theory was applied in a first attempt to identify and model zein microphase behavior.

The Flory-Huggins solution theory gives an expression for  $\Delta G_m$ , the change in Gibbs free energy of mixing a polymer with a solvent<sup>20</sup>

$$\Delta G_m = RT[n_1 \ln \phi_1 + n_2 \ln \phi_2 + n_1 \phi_2 \chi_{12}] \quad (1)$$

where polymer and solvent are labeled 1 and 2, respectively,  $n$  is their number of moles, and  $\phi$  is their volume fraction. The Flory-Huggins parameter,  $\chi$ , takes into account the energy of interdispersing polymer and solvent molecules.  $R$  is the gas constant and  $T$  is the absolute temperature.  $\phi_1$  and  $\phi_2$  are related to  $n_1$  and  $n_2$  by

$$\begin{cases} \phi_1 = \frac{n_1 N_1}{n_1 N_1 + n_2 N_2} \\ \phi_2 = \frac{n_2 N_2}{n_1 N_1 + n_2 N_2} \end{cases} \quad (2)$$

where  $N_1$  and  $N_2$  are the polymerization numbers of polymer and solvent, respectively. In this work,  $N_1 = 1$  because no polymerization reactions are involved<sup>20-22</sup> and  $N_2 = 1$  because the degree of polymerization of solvent is taken as unity for polymer solutions.<sup>23</sup> Therefore, using eq 2, eq 1 can be written as

$$F_{\text{mix}} = k_B T [\phi_1 \ln \phi_1 + \phi_2 \ln \phi_2 + \phi_1 \phi_2 \chi_{12}] \quad (3)$$

where  $F_{\text{mix}}$  is the free energy change of mixing per molecule. Because  $\phi_1 + \phi_2 = 1$  and  $\chi$  is used in place of  $\chi_{12}$ , eq 3 can be further simplified to

$$\frac{F_{\text{mix}}}{k_B T} = \phi_1 \ln \phi_1 + (1 - \phi_1) \ln(1 - \phi_1) + \chi \phi_1 (1 - \phi_1)^2 \quad (4)$$

## 2. Materials and Methods

**2.1. Materials.** Zein was obtained from Showa Sanyo (Tokyo, Japan). Ethanol (190 proof, USP) was from Decon Laboratories (King of Prussia, PA).

**2.2. Evaporation-Induced Self-Assembly.** Zein (0.20–150 mg/mL) was dispersed in a series of ethanol-water mixtures (30–95% (v/v)). We sonicated zein solutions for 2 min using an ultrasonic processor VC-750 (Sonics & Materials, Newtown, CT) operated at 300 W to decrease particle size and improve distribution. Samples of those solutions (10 mL) were placed under the

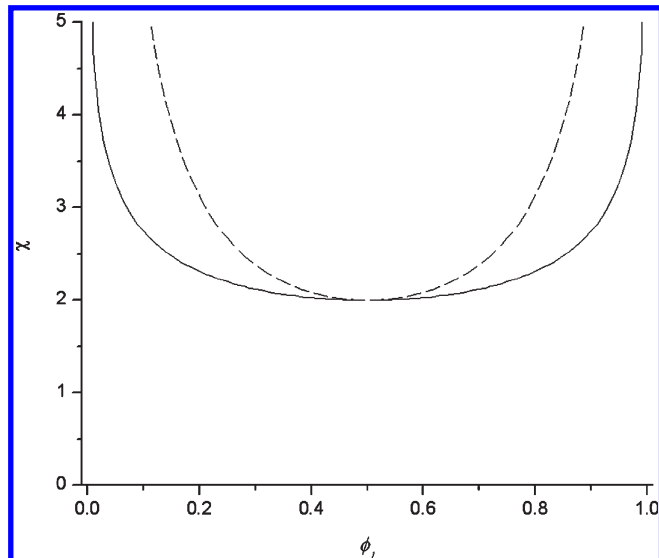


**Figure 1.** Phase diagram of a system described by Flory-Huggins solution theory, derived from eq 4. The solid line represents the condition  $dF_{\text{mix}}/d\phi_1 = 0$ , the dashed line represents  $d^2F_{\text{mix}}/d\phi_1^2 = 0$ .

hood in aluminum dishes to allow evaporation-induced self-assembly (EISA). The ethanol content of the solvent was in every case below the azeotropic point. Therefore, ethanol was expected to evaporate out of the solvent at a faster rate than water, continually increasing the water content and hydrophilic character of the solvent. A hydrophilic environment was expected to promote hydrophobic associations and mediate the self-assembly of zein structures. Evaporated samples were collected and stored at room temperature in constant humidity chambers kept at 80% relative humidity.

**2.3. Scanning Electron Microscopy (SEM).** Dry samples after EISA were gold coated (300 Å) by an Emitech K575 sputter coater (Ashford, U.K.) to help improve electrical conductivity of sample surfaces. SEM images were obtained with a JEOL 6060LV general purpose SEM (Peabody, MA).

**2.4. Focused Ion Beam (FIB) Microscopy.** FEI dual beam 235 FIB (Hillsboro, OR) is a combination of a high-resolution field emission SEM and a scanning metal ion beam microscope. A Ga ion beam was used by the FIB to remove the material on the sample surface in a controlled pattern.

## 3. Results and Discussion

**3.1. Morphology Characterization.** SEM images of evaporated samples are shown in Figures 2–5. Figure 2 shows free microspheres formed from dilute zein solutions (2 mg/mL) in 70% ethanol. Figure 3 shows an FIB image of a sphere cross-section. It was believed that microspheres self-assembled layer-by-layer by adsorption to a central core or nucleus. Radial growth occurred by hydrophobic associations as ethanol evaporated, increasing the water content and hydrophilic character of the solvent. The microspheres diameter reached  $\sim 1 \mu\text{m}$ . Figure 4 shows tightly packed spheres obtained at higher zein concentrations (10 mg/mL). Microsphere diameter reached  $\sim 3 \mu\text{m}$ . In Figure 5, when zein concentration in solution reached 100 mg/mL, microspheres were fused into a film.

EISA is a technique used to promote the self-organization of nanostructures. Petkov and coworkers<sup>25</sup> employed EISA for the formation of mesoporous films from a polyethylene and

(19) Pryamitsyn, V.; Ganesan, V. *J. Chem. Phys.* **2004**, *120*, 5824–5838.

(20) Flory, P. J. *J. Chem. Phys.* **1942**, *10*, 51–61.

(21) Ojeda, J. R.; Mobley, J.; Martin, D. C. *J. Polym. Sci., Part B: Polym. Phys.* **1995**, *33*, 559–569.

(22) Zafarani-Moattar, M. T.; Sadeghi, R. *Fluid Phase Equilib.* **2002**, *202*, 413–422.

(23) Asai, S.; Majumdar, S.; Gupta, A.; Kargupta, K.; Ganguly, S. *Comput. Mater. Sci.* **2009**, *47*, 193–205.

(24) Jones, R. A. L. *Soft condensed Matter*; Oxford University Press: New York, 2002.

(25) Petkov, N.; Mintova, S.; Karaghiosoff, K.; Bein, T. *Mater. Sci. Eng., C* **2003**, *23*, 145–149.

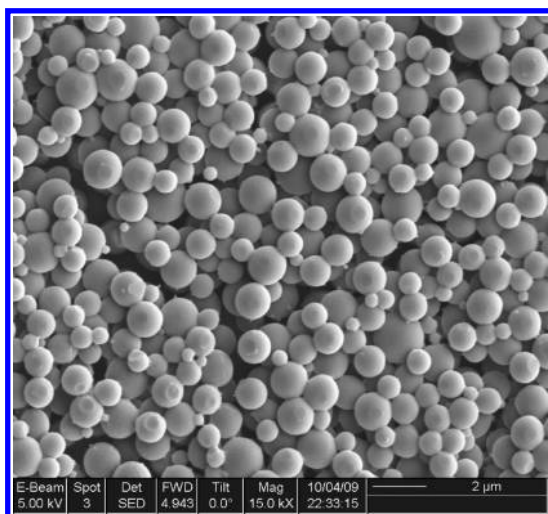


**Figure 2.** SEM image of zein spheres obtained by EISA from a solution containing 2 mg zein/mL 70% ethanol.

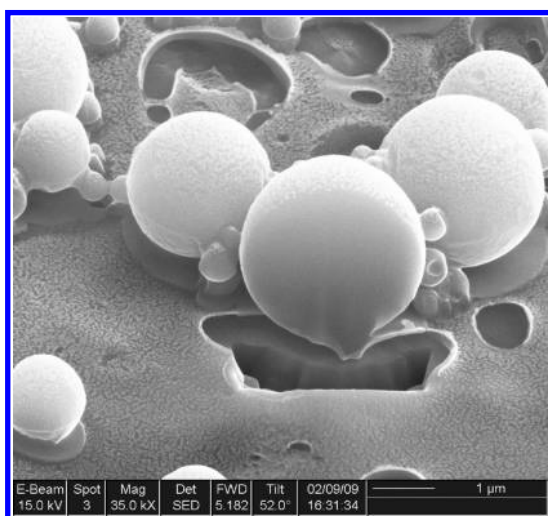


**Figure 3.** Cross section view by FIB of zein spheres obtained by EISA from a solution containing 2 mg zein/mL 70% ethanol.

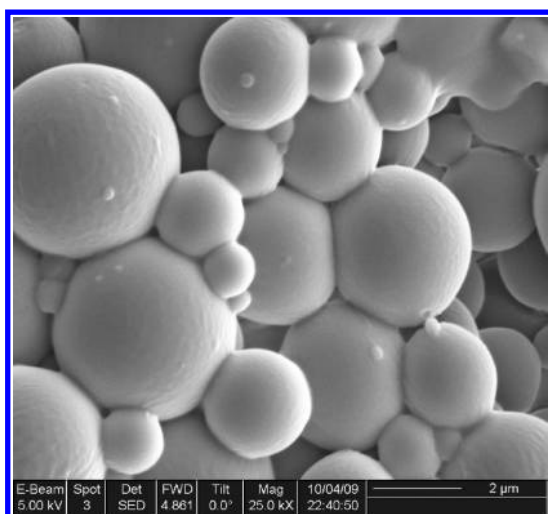


**Figure 4.** SEM image of closely packed zein spheres obtained by EISA from solutions of 10 mg zein/mL 70% ethanol.

polypropylene oxide block copolymer. They observed that solvent evaporation of the coating mixture induced the formation of

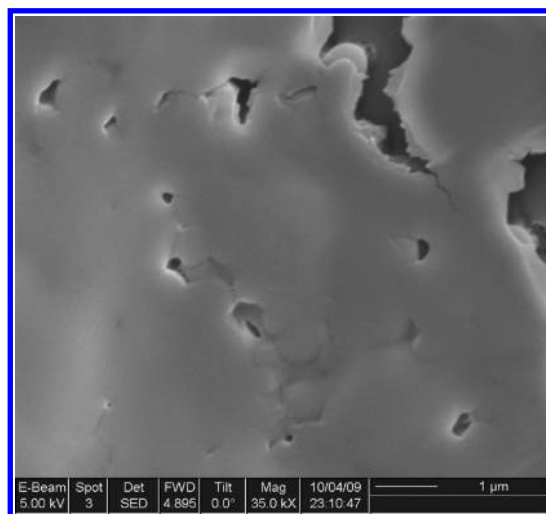


**Figure 5.** SEM image of zein lamellae obtained by EISA from solutions of 100 mg zein/mL 70% ethanol.

3D micellar interiors, which self-assembled into a cubic meso-phase structure. EISA is a nonequilibrium process that is affected by solvent evaporation rates.<sup>26,27</sup> However, under the same experimental conditions, we could obtain different film morphologies by varying the initial concentration of the mother solutions. Colloidal crystals were fabricated by EISA of aqueous colloidal suspensions of silica microspheres. Lu and coworkers<sup>28</sup> obtained various patterns from circular lines to 3D crystals by controlling the concentrations of silica colloidal suspensions from 0.02 to 0.2 wt %. Because EISA processes are difficult to describe by phase diagrams, we sought to gain insight into the effect of mother solution composition on the morphology of EISA deposits by studying the microphase behavior of the solutions.

### 3.2. Microphase Behavior of Zein in Ethanol–Water.

Figure 6 presents a plot of zein volume fraction (1 mg zein  $\approx$  0.82  $\mu$ L) against ethanol concentration in the solvent. Data points (symbols) represent the type of morphology of evaporated samples. It was assumed that the different morphology types of evaporated samples corresponded with different microphases existing in solution.

In the Flory–Huggins solution theory,  $\chi$  is defined as the energy of interdispersing polymer and solvent molecules, which is related to the solubility of the polymer in a solvent. Low  $\chi$  values correspond to high solubility.<sup>29,30</sup>  $\chi$  shows a complex dependence on temperature, concentration, and degree of polymerization.<sup>31,32</sup> Assumptions are usually made on the relations between  $\chi$  and those parameters to simplify their studies.<sup>23</sup> Bouchaour and coworkers,<sup>33</sup> in their study of the phase equilibrium of poly(*n*-butyl acrylate) and the low molecular mass liquid crystal mixture E7, assumed that  $\chi$  and temperature follow the relation

(26) Brinker, C. J.; Lu, Y. F.; Sellinger, A.; Fan, H. Y. *Adv. Mater.* **1999**, *11*, 579–.

(27) Gibaud, A.; Grosso, D.; Smarsly, B.; Baptiste, A.; Bardeau, J. F.; Babonneau, F.; Doshi, D. A.; Chen, Z.; Brinker, C. J.; Sanchez, C. *J. Phys. Chem. B* **2003**, *107*, 6114–6118.

(28) Lu, Y. F.; Ganguli, R.; Drewien, C. A.; Anderson, M. T.; Brinker, C. J.; Gong, W. L.; Guo, Y. X.; Soyze, H.; Dunn, B.; Huang, M. H.; Zink, J. I. *Nature* **1997**, *389*, 364–368.

(29) Wei, Y. M.; Xu, Z. L.; Yang, X. T.; Liu, H. L. *Desalination* **2006**, *192*, 91–104.

(30) Patel, S. K.; Lavasanifar, A.; Choi, P. *Biomaterials* **2010**, *31*, 345–357.

(31) Lee, K. W. D.; Chan, P. K.; Feng, X. S. *Chem. Eng. Sci.* **2004**, *59*, 1491–1504.

(32) Flory, P. J. *Principles of Polymer Chemistry*; Cornell University Press: New York, 1953.

(33) Bouchaour, T.; Benmouna, F.; Leclercq, L.; Ewen, B.; Coqueret, X.; Benmouna, M.; Maschke, U. *Liq. Cryst.* **2000**, *27*, 413–420.

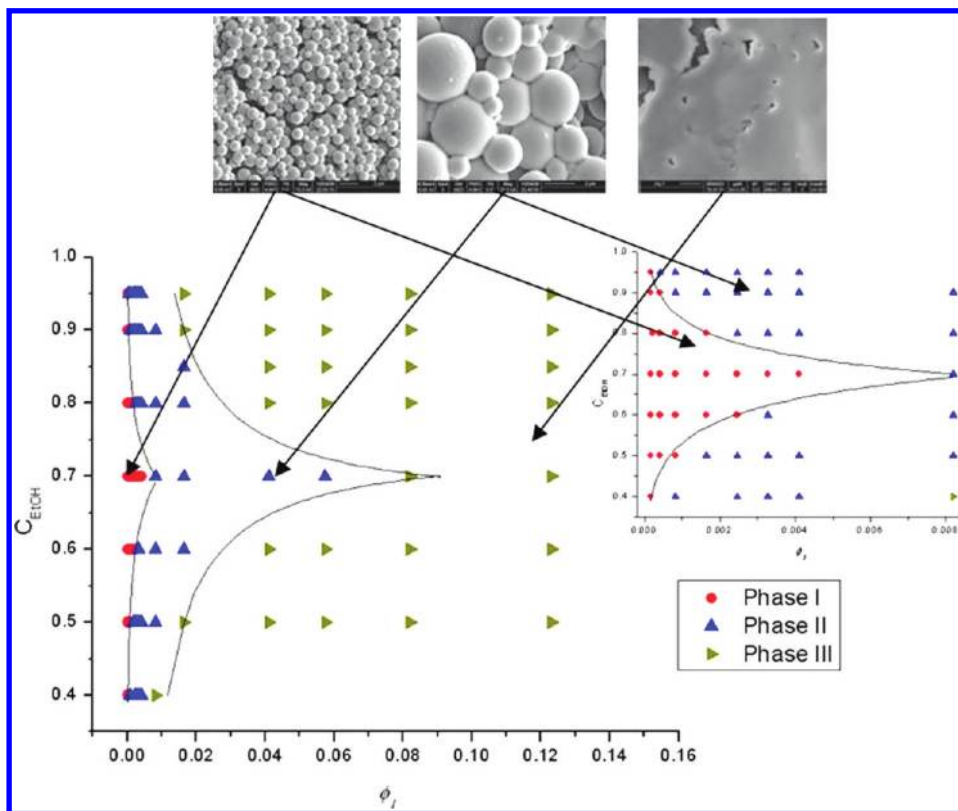


**Figure 6.** Zein microphases in ethanol/water. Symbols represent deposits of similar morphology obtained after solvent evaporation. Solid lines are the microphase boundaries generated by curve fitting of eqs 7 and 8. Inset is an enlarged figure for the  $\phi_1$  range 0 to 0.0085.

$\chi = A + B/T$ , where  $A$  and  $B$  are constants independent of temperature and composition. The relation between  $\chi$  and ethanol concentration in the solvent was based on zein solubility. Figure 7a shows an early ternary phase diagram of zein in ethanol–water (adapted from Mossé<sup>34</sup>), where zein solubility occurs between 50 and 90% ethanol. Phase separation was observed at lower (<40%) or higher (>90%) ethanol concentrations. Shukla and coworkers<sup>35</sup> later investigated the effect of ethanol concentration on zein solubility. They pointed out that zein solubility in ethanol–water has a maximum value at 70% ethanol (v/v) and continually decreases in both directions (Figure 7b).

In this work,  $\chi$  was assumed to have a linear relation with ethanol concentration in the solvent, as follows

$$\begin{cases} \chi = k_1 C_{\text{EtOH}} + b_1 & (k_1 > 0) \text{ if } C_{\text{EtOH}} > 70\% \\ \chi = k_2 C_{\text{EtOH}} + b_2 & (k_2 < 0) \text{ if } C_{\text{EtOH}} < 70\% \end{cases} \quad (5)$$

$C_{\text{EtOH}}$  is proportional to  $\chi$ ,  $k_1 > 0$ , when ethanol concentration is >70% and inverse proportional,  $k_2 < 0$ , when ethanol concentration is <70%.

Equation 6 can be derived from eqs 2 and 5 as follows

$$C_{\text{EtOH}} = \frac{1}{k_{1,2}} \left( \frac{F_{\text{mix}}}{k_B T} - \phi_1 \ln \phi_1 - (1 - \phi_1) \ln(1 - \phi_1) \right) - \frac{b_{1,2}}{k_{1,2}} \quad (6)$$

where

$$\begin{cases} k_{1,2} = k_1 & \text{and } b_{1,2} = b_1 & \text{when } C_{\text{EtOH}} > 70\% \\ k_{1,2} = k_2 & \text{and } b_{1,2} = b_2 & \text{when } C_{\text{EtOH}} < 70\% \end{cases}$$

The boundary lines in the phase diagram, shown in Figure 6, can be derived from eq 6 when conditions are imposed as follows

$$C_{\text{EtOH}} = \frac{P_1 \ln \frac{\phi_1}{1 - \phi_1}}{2\phi_1 - 1} - P_2 \quad \text{when } \frac{dF_{\text{mix}}}{d\phi_1} = 0 \quad (7)$$

and

$$C_{\text{EtOH}} = \frac{P_1}{2\phi_1(1 - \phi_1)} - P_2 \quad \text{when } \frac{d^2 F_{\text{mix}}}{d\phi_1^2} = 0 \quad (8)$$

where  $P_1$  and  $P_2$  represent  $1/k_{1,2}$  and  $b_{1,2}/k_{1,2}$ , respectively.

We investigated the microphase behavior of zein by fitting eqs 7 and 8 to the data presented in Figure 6, corresponding to zein (MW  $\approx$  25 000) solutions of 0.25, 0.5, 1, 2, 3, 4, 5, 10, 20, 50, 75, 100, and 150 mg zein/mL ethanol–water of 30, 40, 50, 60, 70, 80, 85, 90, and 95% v/v. Phase boundary lines were generated by fitting eqs 7 and 8 to the points belonging to the same phase on the boundary region. Table 1 shows the values of the parameters  $P_1$ ,  $P_2$ , and the  $R^2$  values for curve fitting.  $P_1$  values are of the same order of magnitude but opposite signs for each pair of symmetrical curves. (See Figure 6.) Phase boundary lines above  $C_{\text{EtOH}} = 0.7$  resemble those in the model by Matsen and Schick<sup>36</sup> for microphases of diblock copolymers. Below  $C_{\text{EtOH}} = 0.7$ , the boundary lines have mirror symmetry with the upper curves, consistent with the relation between  $\chi$  and  $C_{\text{EtOH}}$ , where  $C_{\text{EtOH}}$  is proportional to  $\chi$  when it is >70% and inversely proportional when it is <70%.  $P_2$  values are negative and of the same order of magnitude for all curves.  $R^2$  values were >0.99, indicating a good fit.

(34) Mossé, J. *Ann. Physiol.* **1961**, 3, 105–139 (in French).

(35) Shukla, R.; Cheryan, M.; DeVor, R. E. *Cereal Chem.* **2000**, 77, 724–730.

(36) Matsen, M. W.; Schick, M. *Phys. Rev. Lett.* **1994**, 72, 2660–2663.

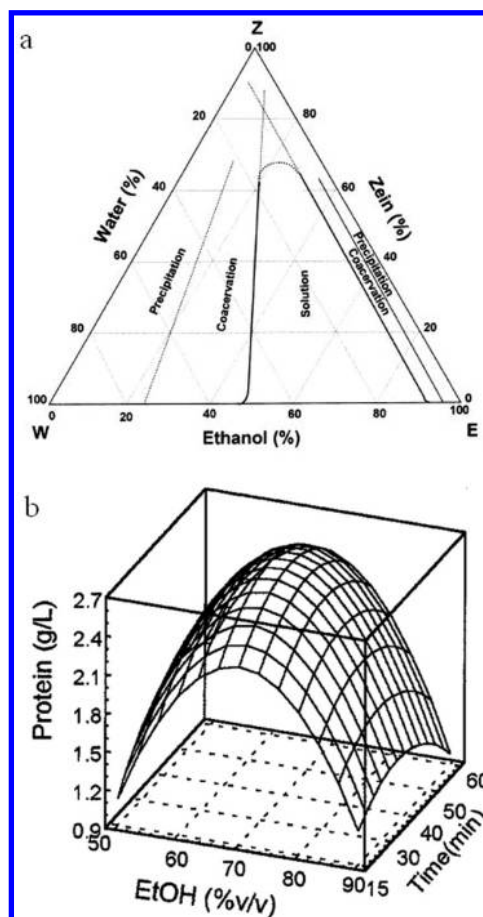


**Figure 7.** (a) Ternary phase diagram of zein in ethanol and water. Adapted from Mossé.<sup>34</sup> (b) Effect of ethanol concentration on zein solubility. Adapted from Shukla.<sup>35</sup>

**Table 1. Curve Fitting Parameters for Phase Boundary Lines Model**

boundary lines	$P_1$	$P_2$	$R^2$
phase I/phase II, $C_{\text{EtOH}} > 70\%$	0.066	-0.37	0.998
phase I/phase II, $C_{\text{EtOH}} < 70\%$	-0.078	-1.07	0.992
phase II/phase III, $C_{\text{EtOH}} > 70\%$	0.008	-0.65	0.999
phase II/phase III, $C_{\text{EtOH}} < 70\%$	-0.008	-0.75	0.999

Figure 6 shows two boundary lines, which defined three regions, attributed to three different microphases. Phase I was considered to be a region of short-range order constituted by dispersed zein monomers, dimers, and structures on the order of 200 nm. Zein discs, 20 nm in diameter and 5 nm in height, and rods, 5 nm in diameter and 200 nm in length, were observed by Wang and coworkers<sup>12</sup> after EISA of zein solutions containing 0.2 mg zein/mL 70% ethanol. At the range considered here, 0.25–5 mg/mL, zein self-assembled into spheres upon solvent evaporation (Figure 2). Figure 3 shows the FIB image of the cross section of a sphere. The interior of the sphere appears to be uniform with no specific structural features. It was hypothesized that zein spheres self-assembled layer-by-layer, growing in an onionskin pattern. This mechanism was also proposed by Conn and coworkers<sup>37</sup> in their study on the dynamics of structural

transformations between phases. Phase II was thought to contain zein aggregates that may have served as cores for the larger spheres observed after EISA. Upon evaporation, spheres packed against each other creating sphere-to-sphere interfaces (Figure 4) and, apparently, a sponge structure. In phase III, zein aggregates may have formed sheets. As the solvent evaporated, they fused together into a continuous film (Figure 5).

Structural transformations resulting from increasing the concentration of components were also reported by other researchers. Schuster and coworkers<sup>38</sup> observed that the mesostructure of the triblock copolymer P123 ( $M_w = 5800$ , EO<sub>20</sub>-PO<sub>70</sub>-EO<sub>20</sub>) changed from a 2D hexagonal mesostructure, to lamellar structure, then to an unknown 3D structure as its concentration increased. Sary and coworkers<sup>39</sup> showed that the rod-coil block copolymer successively self-assembled into spherical, hexagonal, and lamellar phases when the rod volume fraction was increased from 12 to 45%, as observed by TEM. The mechanisms of structural transformations were also studied by model simulations. Shin and coworkers<sup>40</sup> described a model for mesophase assembly of soft-sphere aggregates. According to their model, soft materials arrange into body-centered cubic lattices of sphere aggregates when their concentration is low; as concentration increases, spheres in the lattices approach each other and fuse into a bicontinuous network and then into a lamellar phase. Microphase transitions were discussed by Conn and coworkers,<sup>37</sup> who presented a qualitative model of the transition between bicontinuous and lamellar phases for monoelaidin in excess water based on theories of membrane fusion and existing knowledge of the structure and energetics of bicontinuous cubic phases.

#### 4. Conclusions

Zein concentration and the ethanol–water ratio of the solvent were found to affect largely the morphology of evaporation-induced self-assembled microstructures. Microspheres, packed spheres, and films were observed in the composition ranges studied. The formation of microspheres is of particular interest for the development of delivery systems. Morphology types were mapped on a zein volume fraction–ethanol concentration plane, which revealed a distribution pattern. Such pattern was hypothesized to result from a series of microphases present in the mother solutions. A model based on Flory–Huggins solution theory was fitted to the boundary lines, supporting the presence of proposed microphases. The study generated information on the set of zein concentration–ethanol/water ratio conditions where microspheres are formed and provided insight into the microphase behavior of zein ethanolic solutions.

**Acknowledgment.** We appreciate the help from the Center for Microanalysis of Materials, University of Illinois, which is partially supported by the U.S. Department of Energy under grant DEFG02-91-ER45439.

(37) Conn, C. E.; Ces, O.; Mulet, X.; Finet, S.; Winter, R.; Seddon, J. M.; Templer, R. H. *Phys. Rev. Lett.* **2006**, *96*, 108102.

(38) Schuster, J.; Kohn, R.; Keilbach, A.; Doblinger, M.; Amenitsch, H.; Bein, T. *Chem. Mater.* **2009**, *21*, 5754–5762.

(39) Sary, N.; Brochon, C.; Hadziioannou, G.; Mezzenga, R. *Eur. Phys. J. E* **2007**, *24*, 379–384.

(40) Shin, H. M.; Grason, G. M.; Santangelo, C. D. *Soft Matter* **2009**, *5*, 3629–3638.